Advances in
Geo-Energy Research

Vol. 10, No. 1, p. 21-38, 2023

Invited review

Current methods for measuring three-phase relative permeability and its influencing factors

Yuhao Mei[1,2], Weifeng Lv[1,2,3]*, Xinyu Zhou[3], Jia Huang[3], Ninghong Jia[3], Guo Wang[1,2]

[1] *University of Chinese Academy of Sciences, Beijing 100049, P. R. China*

[2] *Institute of Porous Flow & Fluid Mechanics, Chinese Academy of Sciences, Langfang 065007, P. R. China*

[3] *State Key Laboratory of Enhanced Oil Recovery, Research Institute of Petroleum Exploration and Development, CNPC, Beijing 100083, P. R. China*

Keywords:
Three-phase relative permeability
measurement method
influencing factor
carbon dioxide flooding and storage

Cited as:
Mei, Y., Lv, W., Zhou, X., Huang, J., Jia, N., Wang, G. Current methods for measuring three-phase relative permeability and its influencing factors. Advances in Geo-Energy Research, 2023, 10(1): 21-38. https://doi.org/10.46690/ager.2023.10.04

Abstract:
Three-phase fluid flow in reservoirs is present in the entire process of oil field development, and three-phase relative permeability data are crucial for reservoir engineering and numerical simulation. At the same time, carbon dioxide flooding and storage have garnered significant attention recently. The calculation of dynamic storage volumes and an in-depth understanding of three-phase flow within formations are inextricably linked to three-phase relative permeability. This review is centered around the available experimental measurements, theoretical models that predict three-phase relative permeability using two-phase data, and four Lattice Boltzmann method models. By analyzing the strengths, weaknesses and limitations of each method and assessing the impact of factors like saturation history, interfacial tension, rock properties, and fluid characteristics on three-phase relative permeability, this paper seeks to offer a comprehensive understanding of the topic. In summary, we provide a concise overview of the prospects and challenges in advancing three-phase relative permeability, serving as a valuable reference for the field of carbon dioxide flooding and storage.

1. Introduction

With the development of the petroleum industry, scholars have paid increasing attention to three-phase relative permeability (Alhosani et al., 2021c). Three-phase relative permeability theory was used to describe the flow characteristics of oil, gas and water. It is also useful for reservoir performance calculations in many situations, such as CO_2 flooding, steam flooding, micelle flooding, and nitrogen flooding (Blunt, 2017; Adibifard et al., 2020; Alhosani et al., 2023).

Regrettably, the subject of three-phase relative permeability has garnered significantly less interest than two-phase relative permeability since relevant experimental data was presented in 1941. As such, experimental data on three-phase systems has been limited. The presence of a third phase in the system increases its complexity, which also exponentially raises the time and technology costs (Ahmadloo et al., 2009; Alizadeh and Piri, 2014a; Gupta, 2022; Zankoor et al., 2022). To simplify the calculation process, it is assumed that the relative permeability of the wetting and non-wetting phases is only a single function of their saturation, while the relative permeability of the intermediate phase is a result of the combined effect of the three saturations. Accordingly, a large number of theoretical models for predicting the three-phase data from the two-phase relative permeability data have been derived (Table 1), but none of the model results could be matched exactly with the experimental results (Ahmadloo et al., 2009; Alizadeh and Piri, 2014a). The issue is that these models are unable to reproduce the hysteresis effects and ignore the relationship between saturation paths and saturation histories. Subsequently, many researchers developed new hysteresis models (Land, 1968; Carlson, 1981; Larsen and Skauge, 1998; Kjosavik et al., 2002), but there is still a large gap between their predictions and the laboratory data (Spiteri et al., 2005,

---

Yandy
Scientific
Press

*Corresponding author.
E-mail address: meiyuhao22@mails.ucas.ac.cn (Y. Mei); lweifeng@petrochina.com.cn (W. Lv); zhouxinyu1982@petrochina.com.cn (X. Zhou); j-huang2012@petrochina.com.cn (J. Huang); jianinghong@petrochina.com.cn (N. Jia).

Received August 24, 2023; revised September 14, 2023; accepted October 3, 2023; available online October 8, 2023.

Table 1. Three-phase relative permeability prediction models.

Reference	Model	Theory
Corey et al. (1956)	$k_{ro}=\frac{(S_L-S_w)^3}{(1-S_{Lr})^4}(S_w+S_L-2S_{Lr})$	Extrapolation
Land (1968)	$k_{ro}=S_{of}^{*3}\left[2(S_w^*+s_{of}^*)+S_{of}^*\right]$	Empirical formula
Stone (1970)	$k_{ro}=S_o^*\rho_w\rho_g$	Channel flow, Probabilistic
Stone (1973)	$k_{ro}=(k_{row}+k_{rw})(k_{rog}+k_{rg})-(k_{rw}+k_{rg})$	Channel flow, Probabilistic
Dietrich and Bondor (1976)	$k_{ro}=k_{row}S_w+k_{rog}(S_o+S_w)-k_{ro}^o+\frac{(S_o+S_w)[k_{ro}^o-k_{row}S_w][k_{ro}^o-k_{rog}(S_o+S_w)]}{k_{ro}^o}$	Interpolation
Aziz and Settari (1979)	$k_{ro}=k_{ro}^oS_o^*\rho_w\rho_g$	Normalization
Aziz and Settari (1979)	$k_{ro}=k_{ro}^o\left[\left(\frac{k_{row}}{k_{ro}^o}+k_{rwo}\right)\left(\frac{k_{rog}}{k_{ro}^o}+k_{rgo}\right)-\left(k_{rwo}-k_{rgo}\right)\right]$	Normalization
Baker (1988)	$k_{ro}=\frac{(S_w-S_{wc})k_{ow}+(S_g-S_{gr})k_{rog}}{(S_w-S_{wc})+(S_g-S_{gr})}$	Saturation-weighted interpolation
Delshad and Pope (1989)	$k_{ro}=k_{ro}^o\left[\alpha S_o^*(1-S_w^*)^\beta+(1-\alpha)(S_o^*)^\gamma(1-S_g^*)^\delta\right]$	/
Kokal and Maini (1990)	$k_{ro}=S_o^*\frac{k_{row}}{k_{ro}^o(1-S_w^*)}\frac{k_{rog}}{k_{rg}^o(1-S_g^*)}\frac{k_{rg}^oS_g^*+k_{ro}^oS_w^*}{1-S_o^*}$	Normalization
Hustad and Ransen (1995)	$k_{ro}=\frac{S_w}{S_g+S_w}\widehat{k}_{row}+\frac{S_g}{S_g+S_w}\widehat{k}_{rog}$	Interpolation
Moulu et al. (1997)	$k_{ro}=(S_0+S_{wi})^{\frac{4-D_L}{2-D_L}}-S_{wi}^{\frac{4-D_L}{2-D_L}}$	Poiseuille law
Balbinski et al. (1999)	$k_{ro}=\left(K_{rog}S_{on}\right)^{f(\alpha)}\left(K_{row}S_{on}\right)^{1-f(\alpha)}$	Interpolation
Shahverdi and Sohrabi (2013)	$k_{ro}(S_w,S_g)=\frac{S_o^*}{(1-S_g^*)(1-S_w^*)}(k_{row}k_{rwg}+k_{rog}k_{rgw})$	Multi-flow
Kianinejad et al. (2015)	$k_{ri(z,t)}=\frac{-\mu_i(z,t)\mu_i}{k\left(\frac{\delta P_i(z,t)}{\Delta z}-\rho_ig\right)}$	Darcy-Buckingham law
Shahverdi and Sohrabi (2017)	$k_{ro}=\frac{S_{wo}}{S_{wo}+S_{go}}k_{row}S_{ow}+\frac{S_{go}}{S_{wo}+S_{go}}k_{rog}S_{og}$	Multi-flow
Churchwell and DiCarlo (2018)	$k_{ri}=-\mu_i\left(\frac{k}{\mu_i}\frac{d\varphi_i}{dz}\right)^{-1}$	Darcy's law

Note: D_L represents the linear fractal dimension of the porous medium; k_{ri}^0 represents the endpoint relative permeability of phase i; k_{rij} represents the phase i relative permeability measured in the i-j system; S_{wc} and S_{gr} represent irreducible water saturation and residual gas saturation, respectively; S_i represents the saturation of phase i (water, oil and gas); S_i^* represents normalized saturation; $\beta_i=k_{roi}/(1-S_i^*)$; $\widehat{k}_{rij}$ represents the representative relative permeability of phase i in the i-j system; a_i represents the degree of "oil-ness" of the phase i, b_i represents the degree of "gas-ness" of the phase i; φ_i represents the fluid potential.

2006).

The injection of carbon dioxide into geological formations, which can enhance both oil recovery and storage within reservoirs, has been proved to be an effective means of reducing carbon emissions and mitigating the effects of climate change (Wilberforce et al., 2021; Ji et al., 2023). However, complex three-phase flow is a major challenge that arises with this method (Kong et al., 2021). In the context of geological storage where the transportation and distribution of multiphase fluids occur within the pore medium, the accurate determination of relative permeability of CO_2, water and oil becomes significant. It holds great value in assessing the feasibility of storage projects, evaluating the storage potential of reservoirs, predicting CO_2 flow patterns, understanding CO_2 retention capacity, solubility and migration processes in subsurface reservoirs, as well as assessing the effectiveness of storage operations (Zuo et al., 2014; Zhu et al., 2021). To optimize the storage of CO_2 and maximize oil recovery in reservoirs, it is essential to enhance the understanding of pore-scale physics that govern three-phase flow (Blunt, 2017).

This paper provides a comprehensive review of the existing experimental and numerical methods for determining three-phase relative permeability. It offers a detailed introduction to the theoretical models used to predict three-phase relative permeability based on two-phase data, and conducts a thorough analysis and comparison of the individual strengths and limitations of such models. The influence factors of three-phase relative permeability are systematically analyzed and several suggestions are made for the development of three-phase relative permeability, hoping that three-phase relative permeability can be positively developed.

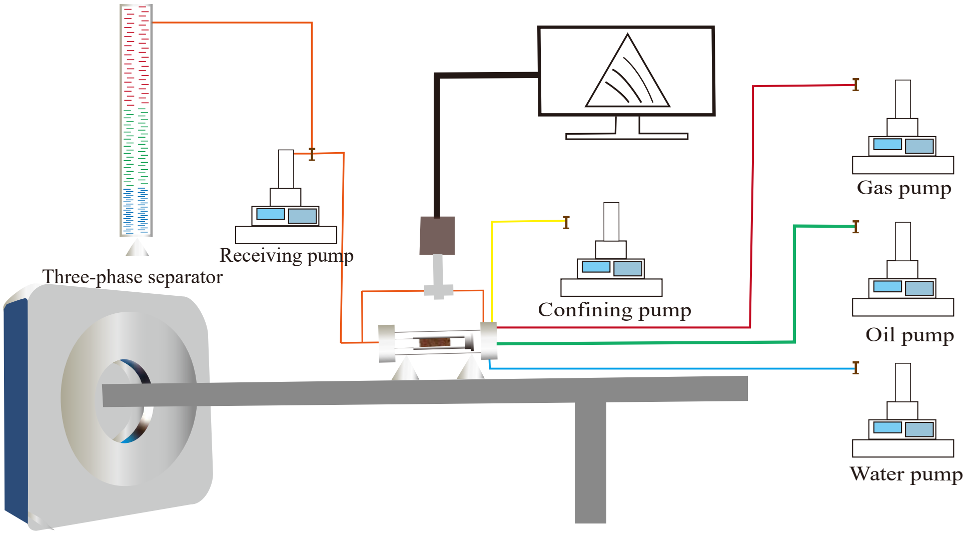

Fig. 1. Steady-state three-phase relative permeability experiment.

2. Experimental methods

2.1 Steady-state methods

The application of different experimental methods under varying flow conditions during the flooding process leads to significant discrepancies in the measured relative permeability curves (Singh et al., 2001), Thus, it is important to recognize that relying on a single approach is insufficient for accurately representing the diverse range of flow regimes encountered in reservoirs, and it is essential to comprehend the various measurement methods available. The steady-state method (Fig. 1) is grounded in Darcy's seepage theory and was initially introduced by Leverett and Lewis (1941):

$$v_i = -\frac{kk_{ri}}{\mu_i}\frac{\partial P_i}{\partial s} \tag{1}$$

where v represents the flow rate per unit cross-sectional area of the porous medium perpendicular to the flow direction; k represents the absolute permeability of rock; k_{ri} represents the relative permeability of phase i; μ_i represents the kinetic viscosity of phase i; $\partial P_i/\partial s$ is the pressure gradient.

Due to its reliance on Darcy's law, the steady-state method yields results that are typically less contentious, provided that end effects can be successfully mitigated (Maini et al., 1989). The advent of computed tomography (CT) scanning technology in recent years has enabled researchers to visualize pore structures and fluid distribution within porous media while conducting steady-state experiments (Yang et al., 2021). This technique has yielded valuable insights into the intricate phenomena of three-phase flow (Alhosani et al., 2021c; Zankoor et al., 2022). The application of three-dimensional X-ray imaging has facilitated the visualization and quantification of fluid flow within micron-sized pore spaces, enabling the analysis of various pore-scale flow properties (Alhosani et al., 2021b; Blunt, 2021a, 2021b).

Numerous scholars have provided comprehensive descriptions of the steady-state experimental procedure (Oak, 1990; Akhlaghinia et al., 2014; Moghadasi et al., 2016). However, the limitations of this method have become increasingly apparent: the experimental process is elaborate, with extensive duration that often exceeds six months to complete a single steady-state experiment. Consequently, many scholars opt to refrain from this approach.

2.2 Unsteady-state methods

While the steady-state method yields results that are generally less disputable (Caudle et al., 1951; Maini et al., 1989), its extended experimental duration has proved challenging for numerous scholars. Thus, a substantial portion of researchers favors the unsteady-state approach due to its cost-effectiveness, simplicity and reduced time requirements (Sarma et al., 1994; Akin and Demiral, 2001; Perez-Carrillo et al., 2008). The unsteady-state method, rooted in the Buckley-Leverett theory, operates under the same underlying assumptions as the steady-state method. In contrast, the unsteady-state approach typically employs single-phase fluid injection in each flooding process, which involves recording the yield of each fluid at the sample outlet and monitoring the pressure difference across the sample over time. The calculation of these parameters relies on the Johnson-Bossler-Naumann (J.B.N.) method (Welge, 1952; Johnson et al., 1959), which assumes that each phase of the fluid is a function of its saturation. On the other hand, the traditional J.B.N. method does not consider the fluid spreading characteristics.

While the Buckley-Leverett (B-L) theory was subsequently extended to encompass three-phase unsteady-state experiments (Sarem, 1966; Grader and O'Meara, 1988), its validation remained elusive due to the absence of *in situ* saturation detection techniques (Siddiqui et al., 1996). The experimental validation of this theory with highly favorable outcomes was only possible when the CT scanning technique was successfully employed in flooding experiments. Saturation distribution in porous media varies both spatially and temporally, giving rise to an unsteady-state process. During unsteady-state experiments, high-rate tests are frequently conducted to mitigate the

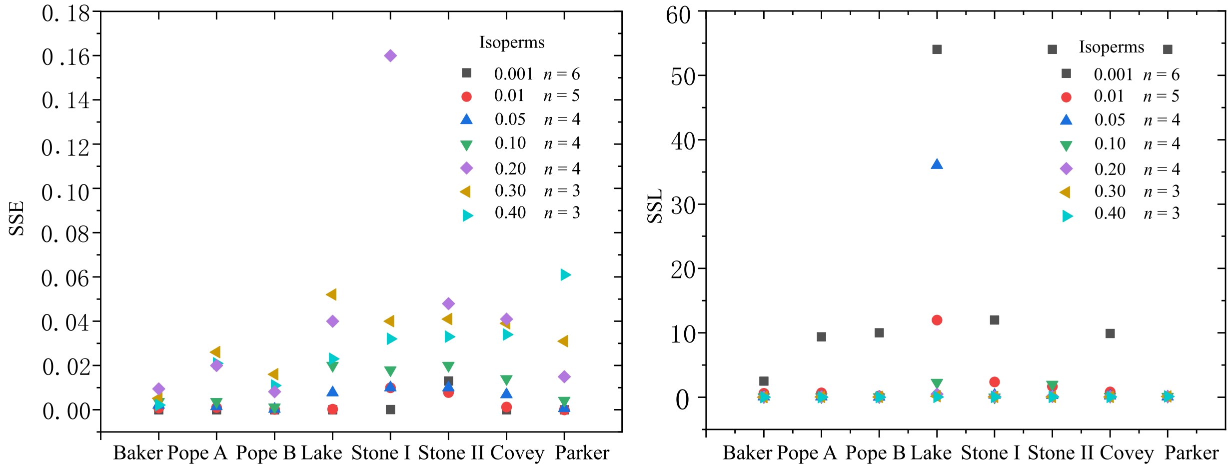

(a) (b)

Fig. 2. Comparison of predicted and experimental data of Corey et al. (1956) using (a) SSL and (b) SSE (Delshad and Pope, 1989).

end effects. Nonetheless, even at elevated replacement rates, the estimated three-phase relative permeability proved to be inaccurate due to inconsistencies with the experimental results, stemming from the linear flow and monotonous saturation variation assumed in the three-phase expansion method in the J.B.N. theory (Akin and Demiral, 2005). Consequently, it is customary to employ more robust methods for data interpretation (Andersen, 2022). The formula for calculating relative permeability was provided by Siddiqui et al. (1998):

$$k_{ri} = -\frac{q_t \mu_i l}{kA} \frac{f_i}{\Delta p - Q\frac{\mathrm{d}(\Delta p)}{\mathrm{d}Q}} \tag{2}$$

where q_t represents the production rate phase i; l represents the core length; A represents the core area; f_i represents the fractional flow of the i-three phase; Δp represents the pressure difference; Q represents flow rate.

3. Theoretical models and empirical correlations

The technique for forecasting three-phase relative permeability was initially introduced by Corey et al. (1956). Initially, it was assumed that water permeability depends solely on water saturation, with the relative permeability of water in a water-wet system equating to that of oil in an oil-wet system. However, this assumption was progressively invalidated. Subsequently, the Corey model was extensively employed for forecasting the relative permeability of the oil phase in three-phase flow, which notably excelled in the prediction of high oil saturation and low oil saturation isoperms. Later, additional scholars introduced their own predictive models (Naar and Wygal, 1961; Land, 1968). The Naar model, for instance, allows for estimating the volume of natural gas confined by water intrusion in gas-oil formations, offering insights into dynamic CO_2 residual trapping. Nevertheless, the applicability of this model is constrained by a scarcity of experimental data. Stone introduced two models, Stone I and Stone II, based on channel flow theory (Stone, 1970, 1973). These models exhibit enhanced predictive capabilities, particularly for water-wet and oil-wet systems, and excel in intermediate oil saturation regions. The prediction of three-phase relative permeability from two-phase data has undergone substantial advancements, resulting in the emergence of various corrective models (Aziz and Settari, 1979; Delshad and Pope, 1989) that achieve strong performance across all regions. Nevertheless, the Stone model has encountered some skepticism as it heavily relies on empirical formulas (Alemán and Slattery, 1988; Moulu et al., 1997; Balbinski et al., 1999) and is predominantly effective in more strongly water-wet cores. In this context, the sum of squares (SSE) and the sum of squared logarithms (SSL) were employed to evaluate the relationships among relative permeability models (Fig. 2) (Delshad and Pope, 1989):

$$\mathrm{SSE} = \sum_n \left[(k_{ro})_e - (k_{ro})_c\right]^2 \tag{3}$$

$$\mathrm{SSL} = \sum_n \left[\log(k_{ro})_e - \log(k_{ro})_c\right]^2 \tag{4}$$

where the subscripts e and c represent experimental and predicted values, respectively; n denotes the number of experimental data points for any specific oil isoperm.

Numerous theoretical models for three-phase relative permeability are available (Table 1). Many of these are derived from limited experimental data, leading to challenges regarding their accuracy and applicability. In general, no single theoretical model can precisely predict the relative permeability for all types of media; therefore, it is of paramount importance to develop a reliable and practical three-phase relative permeability model.

4. Numerical methods

Historically, research on three-phase flow has often depended on solving the Navier-Stokes equations to ascertain the flow parameters, with commonly employed models including the volume-of-fluid, phase-field method, and level-set model. Yet, these models frequently necessitate complex algorithms

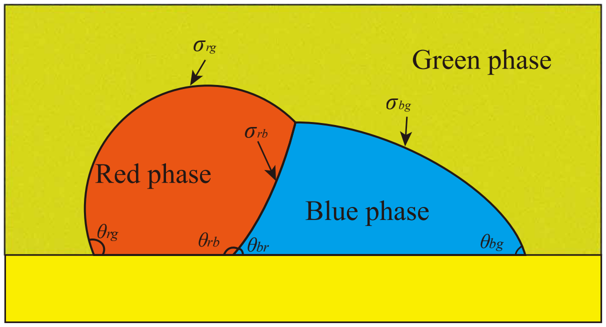

Fig. 3. Two contacting droplets placed on a solid wall.

to accurately capture the fluid interfaces (Zhu et al., 2022b). Furthermore, generating high-quality meshes poses challenges and leads to significant computational resource demands, making them less suitable for simulating porous media such as rocks. As a result, few researchers have employed these methods for simulating three-phase flow processes in rock formations.

The lattice Boltzmann method (LBM), established on microscopic models and mesoscopic dynamics, has gained significant prominence. It offers several distinct advantages over traditional Navier-Stokes equation solution methods, including the capability to address complex boundaries and employ more efficient algorithms. As a result, LBM is swiftly emerging as one of the most frequently employed approaches for addressing multiphase flows (Liu et al., 2015). LBM originates from the lattice gas automata method, thus inherits its numerous advantages. It is well-suited for massively parallel computers due to its temporal and spatial localization. LBM remains under active development; some of the primary models employed for investigating multiphase flow in porous media comprise the color gradient model, the pseudopotential model, the free energy model, and the He-Shan-Doolen model.

The three-phase color gradient model employs various colors to distinguish between fluid phases (Fig. 3) and introduces interfacial tensions between the fluids via the color gradient (Gunstensen, 1992; Spencer et al., 2010). By incorporating the weighted wetting angle (Eq. (5)), it facilitates the computation of multiphase flow in porous media with varying wetting characteristics (Zhang et al., 2016):

$$\begin{aligned} \theta_r &= \frac{C_b}{1-C_r}\theta_{rb} + \frac{C_g}{1-C_r}\theta_{rg} \\ \theta_g &= \frac{C_b}{1-C_g}\theta_{gb} + \frac{C_g}{1-C_g}\theta_{gr} \\ C_b &= 1-C_r-C_g \end{aligned} \tag{5}$$

where θ_i represents the weighted wetting angle of phase i, $i=r,g,b$; θ_{ij} represents wetting angle between phase i-j, $i=r,g,b, j=r,g,b$; C_k denotes the density fraction of k phase defined as $C_k=\rho_k/\rho$, $k=r,g,b$.

Notably, the color gradient model offers several significant advantages, including the flexibility to adjust interfacial tension and its stable performance even at high viscosity ratios (Yu et al., 2019). At present, this model finds application in predicting three-phase relative permeability profiles during immiscible CO_2 flooding and investigating the influence of wettability, capillary number and viscosity ratio on these profiles (Yu et al., 2019; Zhu et al., 2021). Xie et al. (2018, 2020, 2021, 2022) also extended the color gradient model to consider multiphase viscoelastic flows. On the other hand, there are also some limitations of this model, particularly when it comes to addressing the challenge of CO_2 miscibility with crude oil. Nonetheless, it excels in applications involving immiscible flooding.

The pseudopotential model is a versatile tool for simulating multicomponent flows at varying mass and constant temperature, which effectively handles complex boundary conditions in multiphase fluid systems (Shan and Chen, 1993). In previous research, this model has been employed to simulate the relative permeability of two immiscible phases (Li et al., 2005; Huang and Lu, 2009; Dou and Zhou, 2013). This is due to its remarkable efficiency in simulating two-phase flow and its capacity to easily incorporate inter-particle interaction forces and model rock wettability, making it one of the most widely adopted LBM models (Chen et al., 2014). The pseudopotential model consists of the single-component multiphase (SCMP) model and the multicomponent multiphase (MCMP) model (Wei et al., 2018). In SCMP, the phase separation of multiple components is achieved by adding a long-range force based on the van der Waals equation of state to different fluids. However, this approach limits the independent control of physical parameters for other fluids by adjusting the strength of the interaction force, impacting qualitative analysis. Consequently, MCMP is the preferred choice despite some of its drawbacks, such as high spurious currents at the interface, coupling between surface tension and density ratio, thermodynamic inconsistencies, and interfacial divergence caused by high viscosity ratios (Yu and Fan, 2010). Several researchers have addressed these issues by incorporating multiple relaxation time collision operators and Guo's forcing method (Guo et al., 2002). Thus, the pseudopotential model holds great promise for both miscible and immiscible simulations in the carbon dioxide flooding process.

The free energy model, which utilizes free energy flooding to account for interfacial tension effects, has been successfully employed to describe multiphase flow in porous media (Swift et al., 1996; Alpak and Saxena, 2023). Specifically, the MCMP free energy model is frequently utilized in cases where inertial forces can be neglected (Hao and Cheng, 2010; Zhou and Huang, 2023). After optimization, this model allows for independent variation of the interfacial tension and contact angle of the fluid, providing greater flexibility in modeling multiphase flow. Despite its promising capabilities, alongside the He-Shan-Doolen model (He et al., 1998), MCMP is currently underdeveloped and remains infrequently employed in modeling three-phase relative permeability as further refinement and development are still required.

5. Influencing factors

5.1 Saturation history

Saturation history, often referred to as saturation sequence, represents the specific path of saturation that a fluid follows during seepage. In the context of two-phase flow, changes in

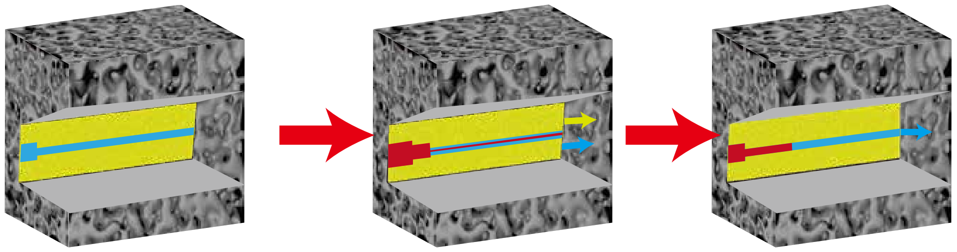

(a) Initial state (b) DDI history (c) DCI history

Fig. 4. A possible path for DDI and DCI saturation history.

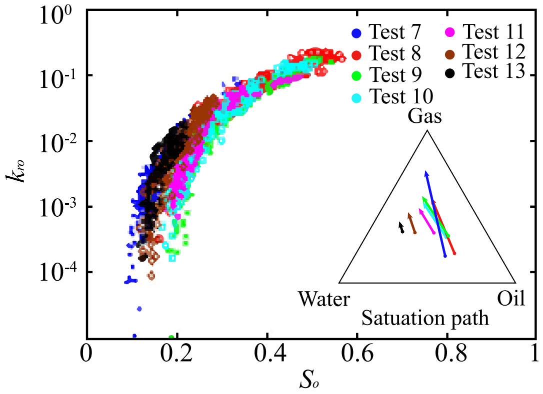

Fig. 5. Relative permeability of the oil phase at different saturation paths (Kianinejad et al., 2015).

the saturation of one fluid inevitably result in changes in the opposite direction for the other fluid. Consequently, the analysis of saturation history in two-phase flow is relatively straightforward. However, in three-phase flow problems, no correlation exists between saturation changes, hence three-phase flow presents a significantly larger number of saturation paths compared to two-phase flow (Carlson, 1981; Blunt, 2000; Lu et al., 2012; Shahrokhi et al., 2014). To more explicitly represent the saturation history, a method has been proposed involving the use of three letters: "D" (Decreasing), "I" (Increasing), and "C" (Constant). These letters are used to indicate the changes in water-oil-gas saturation, with "D" representing a decrease, "I" an increase, and "C" indicating constancy (Oak, 1990). For CO_2 flooding, the primary saturation history patterns observed are "DDI" and "DCI" (Fig. 4). The phenomenon in which different relative permeabilities are observed for the same saturation history undergoing distinct saturation paths is referred to as the relative permeability hysteresis effect, which is commonly observed in three-phase flow systems. Correspondingly, several key hysteresis models have been developed, including the Land hysteresis model (Land, 1968), Killough hysteresis model (Killough, 1976), Carlo hysteresis model (Carlson, 1981), Beattie hysteresis model (Beattie et al., 1989), Larsen hysteresis model (Larsen and Skauge, 1999), and Kjosavik hysteresis model (Kjosavik et al., 2002). It has been demonstrated that different saturation paths within the same saturation history significantly impact the relative permeability of the oil phase, sometimes varying by several orders of magnitude (Fig. 5) (Kianinejad et al., 2015).

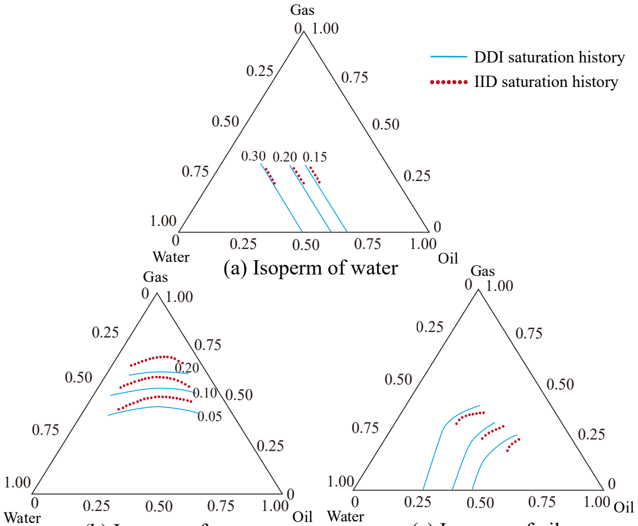

(a) Isoperm of water

(b) Isoperm of gas (c) Isoperm of oil

Fig. 6. Effect of different saturation histories on relative permeability.

The impact of saturation history on three-phase relative permeability exhibits variations, as depicted in Fig. 6. The observed convex curvature of the gas isoperms in the figure contradicts the findings of Stone's model, which suggests that gas relative permeability is solely determined by gas saturation and follows a linear relationship. In the case of immiscible displacement (IID), gas as a non-wetting phase becomes trapped by advancing water and oil. As water and oil saturations increase, a larger proportion of gas transitions into a discontinuous phase, resulting in a decrease in gas relative permeability. Conversely, in the case of drainage displacement (DDI), gas remains in a continuous phase with minimal trapping, leading to a relatively high gas relative permeability that is predominantly influenced by gas saturation. Consequently, compared to IID, the gas isoperms in DDI exhibit a greater curvature and are positioned further away from the 100% gas saturation point, indicating a departure from the linear behavior predicted by Stone's model. Saraf compared the experimental results of unsteady-state and steady-state methods in terms of relative permeability for three-phase gas flow, and found that the relative permeability of the gas phase in unsteady-state conditions is a function of gas saturation and gas saturation history. However, the relative permeability of the water phase exhibits some dispersion without a specific trend, indicating that it is primarily a function of water

Table 2. Three-phase relative permeability for different saturation histories.

Reference	Flow state	Wettability	Saturation history	Media	Gas
Saraf et al. (1982)	steady, unsteady	water-wet	CDI, DCI	Berea	N_2
Grader and O'Meara (1988)	steady	water-wet	DDI	Glass beads	Decane
Maini et al. (1989)	steady	water-wet	IDI, DID	/	N_2
Oak (1990)	steady	water-wet	DDI, IID	Berea	N_2
Oak (1991)	steady	mixed-wet	DDI, IID	Berea	CO_2
Marek et al. (1991)	steady	water-wet	IDI	/	N_2
Eikje et al. (1992)	steady	water-wet	CID, CDI	Berea	/
Kvanvik et al. (1992)	unsteady	mixed-wet	DCI, CID	Berea	/
Dria et al. (1993)	steady	water-wet	DDI	/	CO_2
Muqeem et al. (1993)	steady	water-wet	IDI	Ottawa	N_2
Maloney et al. (1993)	steady	water-wet	DDI	Berea	/
Sarma et al. (1994)	steady, unsteady	water-wet	IDI	/	/
Siddiqui et al. (1996)	steady	water-wet	DDI, IDD	Glass beads	Decane
Kalaydjian et al. (1997)	steady, unsteady	water-wet	CDI	Fontainebleau, Clashach	N_2
Akin and Demiral (1997)	unsteady	mixed-wet	IDI	Berea	N_2
Petersen et al. (2008)	steady	/	DDI, IID	/	gas
Shahverdi et al. (2011a)	steady, unsteady	water-wet, mixed-wet	DCI, DID	Clashach	CH_4, n-C_4
Masihi et al. (2011)	steady	water-wet	IDI	/	N_2
Cao and Siddiqui (2011)	unsteady	water-wet	IDD, DDI, DID	Berea	/
Lu et al. (2012)	steady	water-wet, oil-wet	DDI, IID	/	N_2
Alizadeh and Piri (2014a)	steady	water-wet	DDI	Bentheimer	N_2
Kianinejad et al. (2015)	unsteady	water-wet	DID	Sand pack	air
Kianinejad and DiCarlo (2016)	/	water-wet	DDI	Berea	N_2
Zhang et al. (2018)	steady	water-wet, oil-wet	DDI, IDD	/	CH_4
Alhosani et al. (2021c)	steady	/	DDI, IID	Bentheimer	N_2

saturation and is almost independent of saturation history. The relative permeability of the liquid phase does not show strong dependence on the direction of liquid saturation changes but is influenced by the gas saturation history. In contrast to the unsteady-state method, during steady-state flow, the fluids follow similar paths, resulting in a limited impact of saturation history on relative permeability (Saraf et al., 1982). Maini obtained similar results from steady-state experiments (Maini et al., 1989).

The literature has shown some inconsistency regarding the influence of saturation history on phase permeability, sometimes yielding conflicting results (Alizadeh and Piri, 2014a). Nevertheless, it is now widely acknowledged that the relative permeability of the wetting phase is predominantly governed by its saturation and is minimally impacted by any saturation history. In contrast, the relative permeability of the intermediate and non-wetting phases is influenced by a combination of the saturation levels of each phase and the associated saturation history. For a comprehensive overview of experiments conducted on saturation history over the years, the reader is referred to Table 2.

5.2 Interfacial tension

Throughout the three-phase flow process, numerous interfaces form between each fluid phase as well as between the fluids and rock particles. During this flow, a sequence of physical and chemical interactions unfolds, resulting in interfacial molecular interactions. These in turn lead to capillary phenomena and introduce various additional resistance effects during the seepage process. In CO_2 miscible flooding, a vital factor for enhanced recovery is the formation of a miscible zone at the flooding front (Fig. 10), which strongly hinges on the phase interfacial tension. This also plays a role in the mechanism of carbon dioxide residual trapping (Fig. 7). Substantial evidence suggests that at sufficiently low interfacial tensions, relative permeability is influenced by the ratio of flow

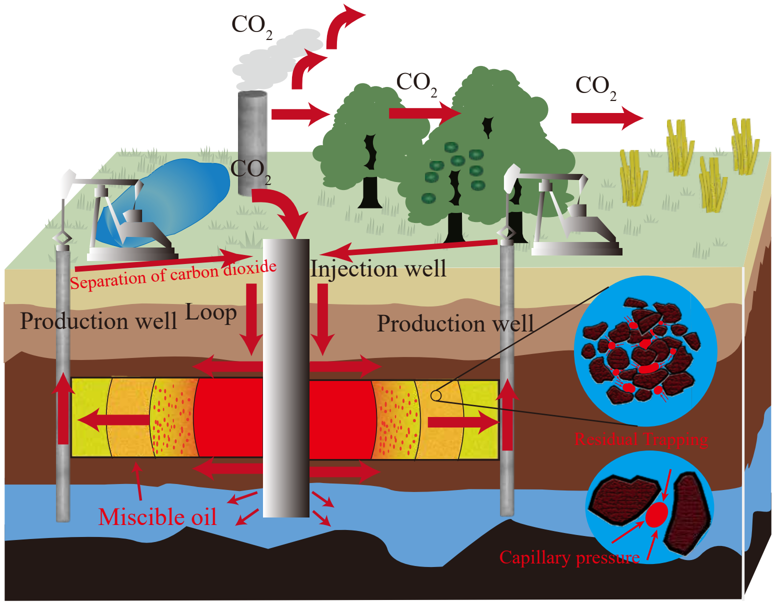

Fig. 7. Carbon dioxide dynamic storage process and the residual trapping mechanism.

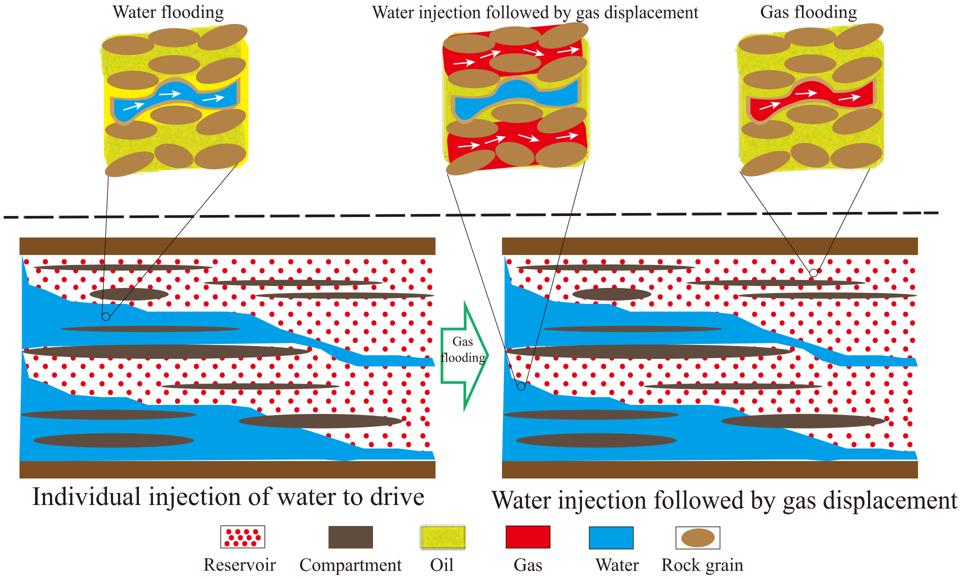

Fig. 8. Gas flooding of oil by avoiding water at low interfacial tension (Li et al., 2021).

rate to interfacial tension (Bardon and Longeron, 1980; Asar and Handy, 1988). Given that low interfacial tension is more likely to occur near the miscible zone at the leading edge, its effect can be quantified by examining the impact of interfacial tension on fluid flow through the lens of the capillary number N_c (Jerauld, 1997):

$$N_c = \frac{k}{\sigma}\left\|\frac{\partial P_i}{\partial s}\right\| \tag{6}$$

where σ represents interfacial tension.

Given the controllable nature of interfacial tension (IFT) within the hydrocarbon/alcohol/water system, extensive research has been conducted to explore the impact of low interfacial tension on the percolation process. Consequently, numerous scholars have carried out three-phase relative permeability experiments under conditions of low interfacial tension (Delshad et al., 1987; Jerauld, 1997). The results consistently indicate that changes in interfacial tension between the nonwetting phases do not affect the relative permeability of the wetting phase, while the relative permeability of the nonwetting phases is notably affected by such changes (Delshad et al., 1987; Kvanvik et al., 1992; Cinar and Orr, 2005; Cinar et al., 2007).

Even though different IFT values do not coincide within the relative permeability saturation range of the oil phase, it has been observed that the residual oil saturation decreases and the relative permeability significantly increases as the gas/oil IFT decreases. This reduction in gas/oil interfacial tension allows gas to bypass water and displace oil (Fig. 8). As water satur-

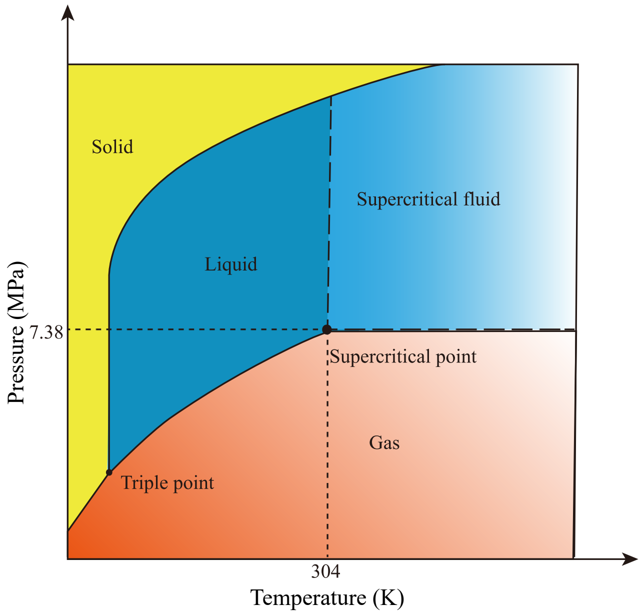

Fig. 9. Carbon dioxide phase diagram.

ation decreases and gas saturation increases, the gas primarily infiltrates pores containing oil and circumvents certain water-filled pores (Jahanbakhsh et al., 2016). During the carbon dioxide flooding process, CO_2 typically infiltrates the reservoir in a supercritical state (Fig. 9), characterized by exceedingly low IFT. This facilitates the displacement of oil by carbon dioxide within minute pores, enabling the retention of carbon dioxide within the pore space. Such behavior can prove advantageous for carbon dioxide flooding applications.

During carbon dioxide flooding operations, when the reservoir pressure reaches the minimum miscible pressure, a miscible zone forms at the leading edge of the displacement process, leading to a significant reduction in the IFT between the two phases. However, it is important to note that earlier experiments were predominantly conducted with nitrogen (Table 2); therefore, the influence of the miscible zone was not accounted for (Fig. 10). As a consequence of the carbon dioxide replacement process, the measurements of three-phase relative permeability exhibited substantial variations due to the impact of the miscible zone at the forefront of the replacement (Dria et al., 1993). In fact, these results sometimes contradicted the assumptions of many empirical models (Shahverdi et al., 2011a). Subsequently, it was revealed that alternating water and gas injection, as well as CO_2 foam drive, can harness the IFT effect, enabling residual oil to flow through the miscible zone and facilitating efficient recovery during subsequent water injection (Mayberry et al., 2008; Tang et al., 2019; Wang et al., 2020).

While it has been firmly established that gas/oil systems with extremely low interfacial tension are nearly miscible (Shelton and Yarborough, 1977), and that CO_2 and crude oil can amalgamate into a single liquid phase under such conditions, it remains uncertain whether ultra-low IFT in surfactant systems is closely associated with miscibility. At present, conclusive data on this matter is lacking.

The influence of IFT on three-phase relative permeability has not yet received adequate attention in the current research. Although the presence of a third phase can significantly alter the magnitude of IFT between the other two phases, limited experiments have measured IFT in the presence of a third fluid phase, while other experiments have mostly overlooked its existence (Alizadeh and Piri, 2014b). Current investigations into interfacial tension systems have primarily focused on water/oil/microemulsion systems, with only a handful of studies delving into the effects of IFT on the dynamics of multiphase fluid flow. In fact, there is a noticeable dearth of literature concerning the impact of IFT on the flow characteristics of oil/gas/water in three-phase flow scenarios.

5.3 Rock wettability

In the context of two-phase flow, rock wettability has a substantial influence on fluid dynamics, and its variations have a pronounced impact on the spatial distribution of oil and water within the pore space. This in turn alters the direction of capillary forces during drainage, ultimately affecting residual oil saturation. While it has been well-established that wettability significantly affects the relative permeability of two phases, there has been limited exploration of this effect on three-phase flow. Divergences in rock wettability notably influence the spatial arrangement of oil and water in the pore space (Fig. 11), subsequently influencing the direction of capillary forces during drainage. The Gussow principle, widely acknowledged as the predominant theory of oil and gas accumulation, has led to a consensus that reservoir rocks are predominantly hydrophilic media. As a result, early investigations into three-phase relative permeability and wettability have predominantly focused on water-wet rocks. Meanwhile, the development of prediction models for three-phase relative permeability has been primarily based on water-wet media (Table 2).

Comprehensive research has unveiled that a significant portion of reservoir rocks do not exhibit pronounced hydrophilic behavior, and notable variations in wettability can exist within various regions of the same reservoir (Brown and Fatt, 1956). Moreover, it has been observed that small pores tend to exhibit water-wet characteristics, whereas larger pores feature considerably lower water wettability (Schmid, 1964; Alhosani et al., 2021a). The first instance of water film rupture was observed in water drive experiments. It was demonstrated that the wettability of the rock surface may alter due to this rupture, leading to mixed wettability behavior (Salathiel, 1973). In turn, an increase in oil-water wettability was linked to a decrease in water saturation. Changes in wettability were also found to correspond to alterations in water-driven recovery, with optimal results occurring when the Amott index approached zero (Jerauld and Rathmell, 1997). Furthermore, various influencing factors were found to exert varying degrees of impact on the three-phase relative permeability in rocks with differing wettability (Skauge and Larsen, 1994; DiCarlo et al., 2000; Cinar et al., 2007; Akindipe et al., 2022). Jerauld's findings revealed that the presence of trapped gas in a mixed-wetted core did not cause a notable decrease in residual oil saturation, which was attributed to the weak mixed wettability of the system. However, the relative permeability of the water

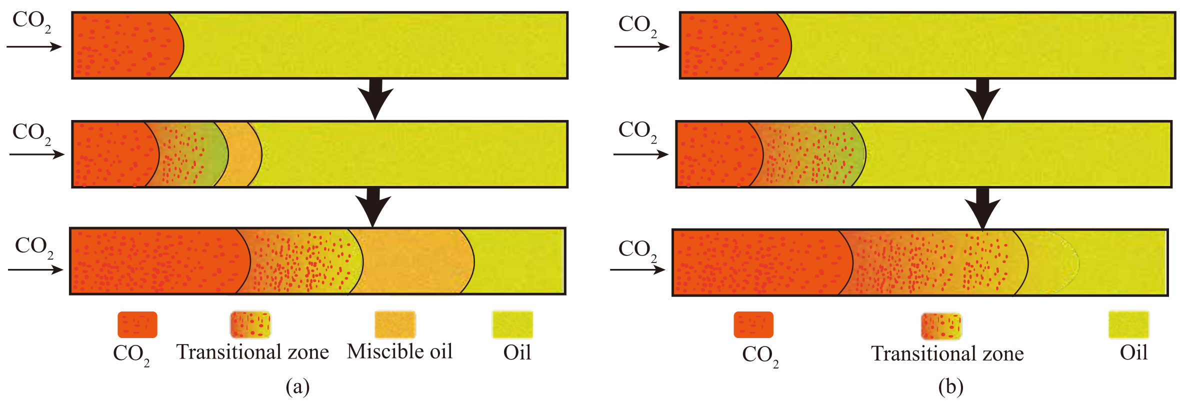

Fig. 10. Carbon dioxide miscible (a) immiscible and (b) process.

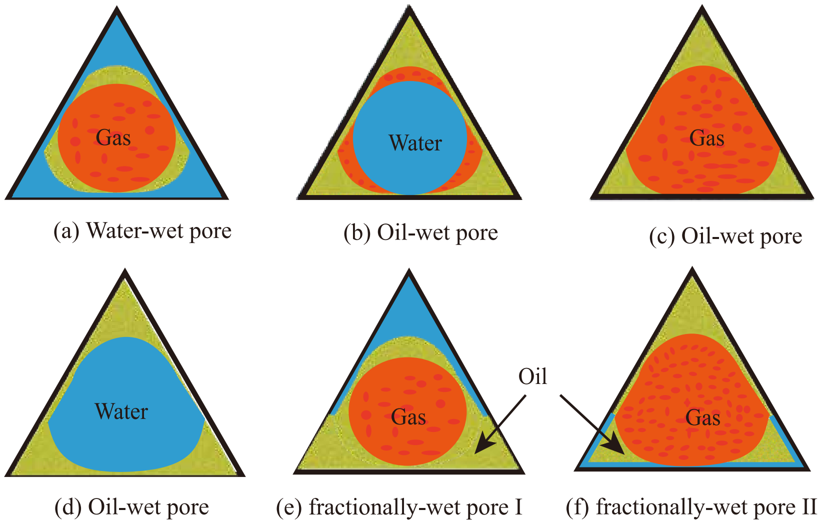

Fig. 11. Configurations of oil, gas and water distribution in triangular pores. (a)Water-wet pore; (b) oil-wet pore with a gas layer; (c) oil-wet pore containing gas; (d) oil-wet pore containing water; (e) fractionally-wet pore I with one oil-wet side; (f) fractionally wet pore II with two oil-wet sides (Zhou and Blunt, 1998).

phase was reduced due to the presence of trapped gas. It is believed that in mixed wetted pores, water and gas compete for larger pores before infiltrating smaller pores due to the lower resistance to flow in the former (Jerauld and Rathmell, 1997).

Under distinct wetting conditions, apart from the varying degrees of influence, the wetting characteristics of each phase differ (Zhou and Blunt, 1998; Hui and Blunt, 2000). In scenarios where CO_2 and crude oil approach miscibility, both substances exhibit intermediate wetting in a water-wet medium, and neither CO_2 nor oil can occupy the central pore space position (Fig. 12), resulting in both having the same pathway for movement (Alhosani et al., 2019).

A strong wetting hysteresis has been observed in the relative permeability of oil, gas and water phase in both mixed-wet and water-wet systems (Shahverdi et al., 2011b). Notably, there is a significant contrast between the results obtained for these two wettability conditions, which also deviates significantly from predictions made by the common three-phase model. However, subsequent experiments conducted by Shahverdi yielded results contradicting his earlier findings (Shahverdi and Sohrabi, 2016). Consequently, it is imperative to garner substantial experimental and theoretical knowledge to enhance the reliability of associated experimental data concerning the influence of rock wettability on three-phase permeability.

5.4 Permeability and pore geometry

For many years, conventional core data have played a fundamental role in determining critical reservoir properties, encompassing total pore storage capacity, permeability distribution, and the permeability of various fluids (Zhu et al., 2022a). After an extensive period of research, it became evident that the relative permeability of a fluid is influenced not only by factors like phase saturation and saturation history but also by the physical attributes of the porous medium through which the fluid flows (Kvanvik et al., 1992; Munkerud and Hoimyr, 1995; Shahverdi and Sohrabi, 2013). While the extent of this dependency on three-phase relative permeability has not been studied extensively, it is believed that the characteristics of the porous media can influence saturation envelopes and al-

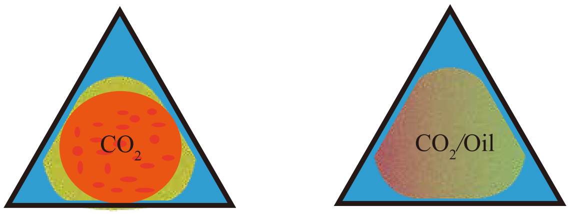

(a) immiscible state (b) miscible state

Fig. 12. Distribution of oil, CO_2 and water in immiscible and miscible displacement.

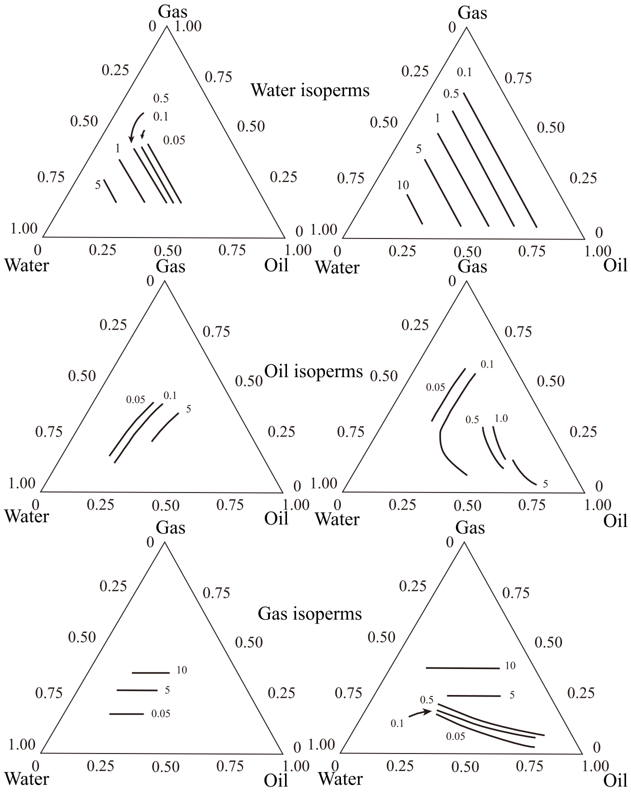

Fig. 13. Three-phase relative permeability results for the Berea (left) and Bentheimer (right) sandstones (Maloney et al., 1990).

ter their sizes in ternary saturation diagrams (Grader and O'Meara, 1988). Beyond the inherent non-uniformity in permeability distribution within the reservoir, the intricate spatial arrangements of pore space are also dictated by the capillary dimensions and tortuosity of the rock (Fatt, 1966; Morgan and Gordon, 1970; Grader and O'Meara, 1988; Maloney et al., 1989; Dernaika and Masalmeh, 2019). Both micropores and macropores exert a significant influence on three-phase relative permeability (Fig. 13). The relative permeability of water in these two cores is solely determined by water saturation. Bentheimer sandstone, however, exhibits lower irreducible water saturation and a larger envelope. At high water saturation, the relative permeability of this kind of sandstone is twice that of Berea sandstone. This difference can be attributed to the presence of a greater number of micropore pores in Berea Sandstone, which imparts higher resistance to water flow through the pores. Regarding the oil-phase isoperms, those of Bentheimer sandstone exhibit concavity towards the oil-phase apex at low gas saturation, indicating a stronger dependence of oil-phase relative permeability on gas-phase saturation. Moreover, the oil-phase relative permeability experiences a pronounced decrease with increasing gas saturation, which may be associated with the abundance of medium-sized pores in this sandstone.

5.5 Fluid spreading characteristics

The spreading behavior of oil film occurs when a gas phase occupies the central region of the pore space, causing the oil phase to form a thin layer positioned between the gas and water phases (Fig. 14). This thin oil film is referred to as spreading layer and is typically just a few microns thick. The presence of this layer ensures hydraulic continuity for the respective phases, enabling flow even at very low saturation levels (Dumore and Schols, 1974). Due to this phenomenon, there has been a resurgence of interest in research on the generation and flow mechanisms of these films (Kantzas et al., 1988). Recent observations have highlighted that water-wet media tend to promote the formation of oil films, resulting in exceptionally low oil-bearing saturation (Kalaydjian, 1992; Kalaydjian et al., 1993). Particularly in strongly water-wet conditions, the flow of oil and water films exerts a significant influence on the oil recovery efficiency of positively spreading systems (Oren and Pinczewski, 1991).

In the presence of gas, the spreading coefficient (K) of oil on water can be elucidated through the balance of interfacial tensions (Adamson and Gast, 1967):

$$K = \sigma_{wg} - (\sigma_{wo} - \sigma_{og}) \tag{7}$$

where subscript w, g and o represent water, gas and oil, respectively.

$K > 0$ indicates that oil will form a spreading film on the water phase, allowing for the continuous flow of both oil and water through the film. Conversely, if $K < 0$, no oil film forms and only water can flow (Oren et al., 1992). The mathematical representation of the contact angle between oil and water is given by the following equation:

$$\cos\theta = 1 + \frac{K}{\sigma_{og}} \tag{8}$$

Under the above definition, in an oil/gas/water system, only one of the three phases can exhibit spreading behavior, while the other two must remain non-spreading at the interface. When none of the fluids exhibit spreading behavior at the interface with the other two fluid phases, it is termed as a non-spreading three-phase system. In cases where all three phases are present in the pore space, the static equilibrium or spatial arrangement of the fluids can be described in three forms (Grattoni et al., 1997). The spreading coefficient of oil on water plays an important role in fluid distribution and recovery in water-wetted and partially wetted porous media. Conversely, in oil-wetting porous media, the spreading coefficient does not significantly impact the flooding efficiency, while the spreading coefficient of water on oil alters fluid distribution in the core (Vizika and Lombard, 1996; Sahni et al., 1998).

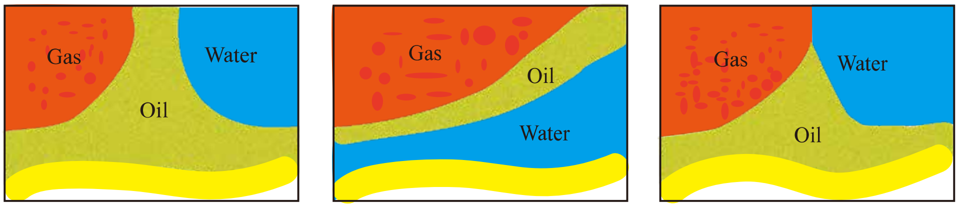

(a) (b) (c)

Fig. 14. Three forms of fluid spreading: (a) Wetting phase spreading; (b) non-wetting phase spreading; (c) non-spreading.

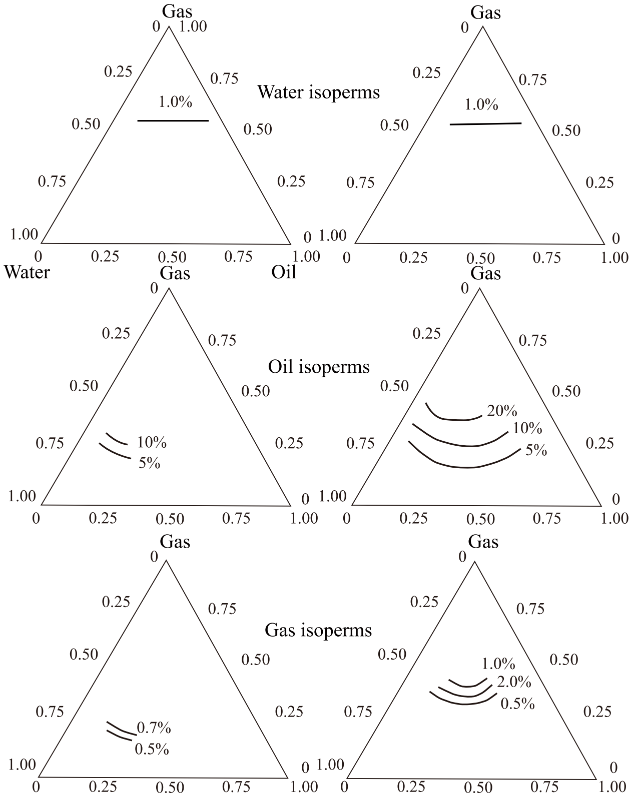

Fig. 15. The comparison of three-phase relative permeability curves between a low and a high oil-phase viscosity system.

5.6 Fluid viscosity

Initially, it was widely accepted that the two-phase viscosity ratio has no impact on relative permeability. However, subsequent research revealed that factors such as capillary number, fluid viscosity and interfacial tension can indeed modulate it (Delshad, 1981). For non-wetting phases with particularly high viscosities, the relative permeability of the non-wetting phase increases with the rising viscosity ratio between the non-wetting phase and the wetting phase. Interestingly, the relative permeability of the wetting phase appears to be unaffected by changes in the viscosity ratio (Zhang et al., 2019). However, it is worth noting that despite the viscosity ratio increasing, the relative permeability of the wetting phase elevates significantly, while the relative permeability of the non-wetting phase remains relatively stable. This suggests that the primary factor driving the change in relative permeability is likely the viscosity of the fluid rather than its wettability (Zhu et al., 2021).

Maloney conducted a study to investigate the impact of viscosity on the relative permeability of Berea sandstone. This involved varying the viscosity of both the oil and brine phases (Fig. 15). The experimental results revealed that the relative permeability of the gas phase is influenced by the saturation of oil and is significantly lower in the presence of higher-viscosity oil. This phenomenon was attributed to the occurrence of plug flow within the gas phase and a change in the interfacial tension between oil and water, and it was concluded that the observed effects cannot be solely attributed to changes in viscosity (Maloney et al., 1989). As the pore space increases, the impact of viscosity ratio tends to decrease significantly and becomes negligible when the permeability exceeds 1,000 mD. This phenomenon can be explained by the Coton's water film theory, that is, a higher viscosity of the non-wetting phase leads to a motion that resembles sliding, thereby increasing its relative permeability (Derjaguin et al., 1987).

6. Challenges and prospects

6.1 Challenges

Although the concept of three-phase relative permeability was introduced almost 100 years ago, several factors have contributed to the limited attention to this field. Firstly, the experimental methods for measuring three-phase relative permeability are constrained by excessive complexity, long duration, and the need for extended steady-state experiments, lasting up to half a year or more. Secondly, in practical engineering applications, the accuracy of predicting three-phase relative permeability using two-phase data often suffices for production needs, which reduces the demand for more precise three-phase data. Consequently, progress in three-phase relative permeability experimental measurement technology has stagnated. Additionally, despite advancements in computer technology, developments in numerical simulation studies on three-phase relative permeability have been scarce. The application of traditional computational fluid dynamics industry methods in porous media encounters obstacles such as modeling challenges, mesh quality issues, and high computational resource requirements, hampering growth in this field.

6.2 Prospects

The rapid development of carbon capture, utilization and storage (CCUS) technology has been driven by the implementation of carbon peaking and carbon neutrality policies. This technology encompasses various aspects, including the injection of carbon dioxide into high-water-content reservoirs in the late stages of development and the critical area of carbon dioxide storage in deep carbon reduction efforts. The relative permeability of three phases plays a pivotal role in both CO_2 flooding and storage, which often occur concurrently. Carbon dioxide storage is a dynamic process, particularly concerning residual trapping, making the calculation of storage volume equally complex. The subsurface flow capacity of oil, CO_2 and water can be characterized by three-phase relative permeability, making it invaluable for calculating dynamic residual trapping. Exciting developments in microscale imaging technology and mesoscopic kinetic methods, such as LBM, have facilitated progress in three-phase relative permeability studies, offering alternatives to time-consuming experiments. Notably, the pseudopotential model has shown great potential in simulating miscible displacement, an important aspect of CCUS. It is essential to recognize that many prior prediction models are based on experiments conducted in water-wet conditions using nitrogen as the replacement gas; however, given that carbon dioxide exhibits miscibility with crude oil, it is imperative to consider three-phase relative permeability within the context of CCUS.

7. Conclusions

The concept of three-phase relative permeability has existed since the 1940s, while the measurement technology in this domain has remained largely stagnant. Therefore, this field requires urgent improvements, necessitating the involvement of more researchers to drive its conscientious development. To address these challenges, the author proposes four key suggestions:

1) Enhancing experimental data: Experimental data serve as the foundation for three-phase prediction models and numerical simulation technologies. Hence, the primary focus should be on overcoming the limitations of existing steady-state and unsteady-state measurement methods, which entails either refining current techniques or exploring innovative experimental approaches. The ideal objective is to reduce experimental cycles and streamline processes, generating substantial data to advance both prediction models and numerical simulations.
2) Consideration of third phase: Emerging evidence indicates that the presence of a third phase can influence the magnitude of two-phase interfacial tension. However, most experiments continue to measure surface tension under conditions involving only two-phase fluids. This practice inevitably impacts experimental outcomes, particularly at interfaces involving CO_2 and crude oil.
3) Quantitative rock wettability assessment: As discussed in Section 4 regarding rock wettability, it is essential to recognize that rock wettability is not uniform and can shift during an experiment. The current rock wettability assessments are qualitative and lack quantitative evaluations, which can lead to anomalous experimental results.
4) LBM pseudopotential model for CO_2 flooding: The pseudopotential model within LBM offers promising capabilities in regulating the miscible region at the flooding front. This model is well-suited for CO_2 miscible flooding and holds substantial development prospects.

Acknowledgements

This work is supported by Joint Fund Program of the National Natural Science Foundation of China (No. U22B6004), and the Prospective and Fundamental Project of CNPC “Digital Rock Center Technology Research” (No. 2021DJ0902).

Additional information: Author’s email

wangguo23@mails.ucas.ac.cn (G. Wang).

Conflict of interest

The authors declare no competing interest.

References

Adamson, A. W., Gast, A. P. Physical chemistry of surfaces, in Geochemistry of Colloid Systems, edited by S. Yariv and H. Cross, Springer Berlin, Heidelberg, pp. 93-155, 1967.

Adibifard, M., Talebkeikhah, M., Sharifi, M., et al. Iterative Ensemble Kalman Filter and genetic algorithm for automatic reconstruction of relative permeability curves in the subsurface multi-phase flow. Journal of Petroleum Science and Engineering, 2020, 192: 107264.

Ahmadloo, F., Asghari, K., Jamaloei, B. Y. Experimental and theoretical studies of three-phase relative permeability. Paper SPE 124538 Presented at the SPE Annual Technical Conference and Exhibition, New Orleans, Louisiana, 4-7 October, 2009.

Akhlaghinia, M., Torabi, F., Chan, C. W. Experimental investigation of temperature effect on three-phase relative permeability isoperms in heavy oil systems. Fuel, 2014, 118: 281-290.

Akin, S., Demiral, M. R. B. Effect of flow rate on imbibition three-phase relative permeabilities and capillary pressures. Paper SPE 38897 Presented at the SPE Annual Technical Conference and Exhibition, San Antonio, Texas, 5-8 October, 1997.

Akin, S., Demiral, M. R. B. Effect of flow rate on imbibition three-phase relative permeabilities and capillary pressures. Energy Sources, 2001, 23(2): 127-135.

Akin, S., Demiral, M. R. B. Limitations of three-phase Buckley-Leverett theory. Energy Sources, 2005, 27(9): 857-865.

Akindipe, D., Saraji, S., Piri, M. Salt precipitation in carbonates during supercritical CO_2 injection: A pore-scale experimental investigation of the effects of wettability and heterogeneity. International Journal of Greenhouse Gas Control, 2022, 121: 103790.

Alemán, M. A., Slattery, J. C. Estimation of three-phase relative permeabilities. Transport in Porous Media, 1988, 3: 111-131.

Alhosani, A., Bijeljic, B., Blunt, M. J. Pore-scale imaging and analysis of wettability order, trapping and displacement in three-phase flow in porous media with various wettabilities. Transport in Porous Media, 2021a, 140: 59-84.

Alhosani, A., Lin, Q., Scanziani, A., et al. Pore-scale characterization of carbon dioxide storage at immiscible and near-miscible conditions in altered-wettability reservoir rocks. International Journal of Greenhouse Gas Control, 2021b, 105: 103232.

Alhosani, A., Scanziani, A., Lin, Q., et al. In situ pore-scale analysis of oil recovery during three-phase near-miscible CO_2 injection in a water-wet carbonate rock. Advances in Water Resources, 2019, 134: 103432.

Alhosani, A., Selem, A., Foroughi, S., et al. Steady-state three-phase flow in a mixed-wet porous medium: A pore-scale X-ray microtomography study. Advances in Water Resources, 2023, 172: 104382.

Alhosani, A., Selem, A. M., Lin, Q., et al. Disconnected gas transport in steady-state three-phase flow. Water Resources Research, 2021c, 57(12): e2021WR031147.

Alizadeh, A. H., Piri, M. The effect of saturation history on three-phase relative permeability: An experimental study. Water Resources Research, 2014a, 50(2): 1636-1664.

Alizadeh, A. H., Piri, M. Three-phase flow in porous media: A review of experimental studies on relative permeability. Reviews of Geophysics, 2014b, 52(3): 468-521.

Alpak, F. O., Saxena, N. An accelerated process-based method for the accurate computation of relative permeability from direct simulations of two-phase flow on micro-computed tomography images of porous media. Journal of Petroleum Science and Engineering, 2023, 220: 111095.

Andersen, P. Ø. Comparison of intercept methods for correction of steady-state relative permeability experiments for capillary end effects. SPE Reservoir Evaluation & Engineering, 2022, 25(4): 882-899.

Asar, H., Handy, L. L. Influence of interfacial tension on gas/oil relative permeability in a gas-condensate system. SPE Reservoir Engineering, 1988, 3(1): 257-264.

Aziz, K., Settari, A. Petroleum Reservoir Simulation. Pennsylvania, USA, Society of Petroleum Engineers, 1979.

Baker, L. Three-phase relative permeability correlations. Paper SPE 17369 Presented at the SPE Enhanced Oil Recovery Symposium, Tulsa, Oklahoma, 16-21 April, 1988.

Balbinski, E., Fishlock, T., Goodyear, S. G., et al. Key characteristics of three-phase oil relative permeability formulations for improved oil recovery predictions. Petroleum Geoscience, 1999, 5(4): 339-346.

Bardon, C., Longeron, D. Influence of very low interfacial tensions on relative permeability. Society of Petroleum Engineers Journal, 1980, 20(5): 391-401.

Beattie, C., Boberg, T., McNab, G. S. Reservoir simulation of cyclic steam stimulation in the Cold Lake oil sands. Paper SPE 18752 Presented at the SPE California Regional Meeting, Bakersfield, California, 5-7 April, 1989.

Blunt, M. J. An empirical model for three-phase relative permeability. SPE Journal, 2000, 5(4): 435-445.

Blunt, M. J. Multiphase Flow In Permeable Media: A Pore-Scale Perspective. Cambridge, UK, Cambridge University Press, 2017.

Blunt, M. J., Alhosani, A., Lin, Q., et al. Determination of contact angles for three-phase flow in porous media using an energy balance. Journal of Colloid and Interface Science, 2021, 582: 283-290.

Brown, R. J., Fatt, I. Measurements of fractional wettability of oil fields' rocks by the nuclear magnetic relaxation method. Paper SPE 743 Presented at the Fall Meeting of the Petroleum Branch of AIME, Los Angeles, California, 14-17 October, 1956.

Blunt, M. J., Kearney, L., Alhosani, A., et al. Wettability characterization from pore-scale images using topology and energy balance with implications for recovery and storage. Paper SPE 206202 Presented at the SPE Annual Technical Conference and Exhibition, Dubai, UAE, 21-23 September, 2021.

Cao, P., Siddiqui, S. Three-phase unsteady-state relative permeability measurements in consolidated cores using three immisicible liquids. Paper SPE 145808 Presented at the SPE Annual Technical Conference and Exhibition, Denver, Colorado, USA, 30 October-2 November, 2011.

Carlson, F. M. Simulation of relative permeability hysteresis to the nonwetting phase. Paper SPE 10157 Presented at the SPE Annual Technical Conference and Exhibition, San Antonio, Texas, 4-7 October, 1981.

Caudle, B. H., Slobod, R., Brownscombe, E. R. Further developments in the laboratory determination of relative permeability. Journal of Petroleum Technology, 1951, 3(5): 145-150.

Chen, L., Kang, Q., Mu, Y., et al. A critical review of the pseudopotential multiphase lattice Boltzmann model: Methods and applications. International Journal of Heat and Mass Transfer, 2014, 76: 210-236.

Churchwell, L., DiCarlo, D. Measuring relative permeability in cores at reservoir pressures using a gravity drainage method. Paper SPE 190322 Presented at the SPE Improved Oil Recovery Conference, Tulsa, Oklahoma, USA, 14-18 April, 2018.

Cinar, Y., Marquez, S., Orr, F. M. Effect of IFT variation and wettability on three-phase relative permeability. SPE Reservoir Evaluation & Engineering, 2007, 10(3): 211-220.

Cinar, Y., Orr, F. M. Measurement of three-phase relative permeability with IFT variation. SPE Reservoir Evaluation & Engineering, 2005, 8(1): 33-43.

Corey, A. T., Rathjens, C., Henderson, J. H., et al. Three-phase relative permeability. Journal of Petroleum Technology, 1956, 8(11): 63-65.

Delshad, M. Measurement of relative permeability and dispersion for micellar fluids in Berea rock. Austin, University of Texas at Austin, 1981.

Delshad, M., Delshad, M., Pope, G. A., et al. Two-and three-phase relative permeabilities of micellar fluids. SPE Formation Evaluation, 1987, 2(3): 327-337.

Delshad, M., Pope, G. A. Comparison of the three-phase oil relative permeability models. Transport in Porous Media, 1989, 4: 59-83.

Derjaguin, B. V., Churaev, N. V., Muller, V. M. Surface Forces. New York, USA, Springer, 1987.

Dernaika, M., Masalmeh, S. The effect of pore geometry on relative permeability in mixed-wet carbonate reservoirs in Abu Dhabi. Paper SPE 197427 Presented at the Abu Dhabi International Petroleum Exhibition & Conference, Abu Dhabi, UAE, 11-14 November, 2019.

DiCarlo, D. A., Sahni, A., Blunt, M. J. Three-phase relative permeability of water-wet, oil-wet, and mixed-wet sandpacks. SPE Journal, 2000, 5(1): 82-91.

Dietrich, J. K., Bondor, P. L. Three-phase oil relative permeability models. Paper SPE 6044 Presented at the SPE Annual Fall Technical Conference and Exhibition, New Orleans, Louisiana, 3-6 October, 1976.

Dou, Z., Zhou, Z. Numerical study of non-uniqueness of the factors influencing relative permeability in heterogeneous porous media by lattice Boltzmann method. International Journal of Heat and Fluid Flow, 2013, 42: 23-32.

Dria, D., Pope, G., Sepehrnoori, K. Three-phase gas/oil/brine relative permeabilities measured under CO_2 flooding conditions. SPE Reservoir Engineering, 1993, 8(2): 143-150.

Dumore, J., Schols, R. Drainage capillary-pressure functions and the influence of connate water. Society of Petroleum Engineers Journal, 1974, 14(5): 437-444.

Eikje, E., Jakobsen, S. R., Lohne, A., et al. Relative permeability hysteresis in micellar flooding. Journal of Petroleum Science and Engineering, 1992, 7(1-2): 91-103.

Fatt, I. Microscopic heterogeneity in reservoir rock and its influence on reservoir behavior. Journal of the Institute of Petroleum, 1966, 52(511): 231-235.

Grader, A. S., O'Meara, D. J. Dynamic displacement measurements of three-phase relative permeabilities using three immiscible liquids. Paper SPE 18293 Presented at the SPE Annual Technical Conference and Exhibition, Houston, Texas, 2-5 October, 1988.

Grattoni, C. A., Almada, M. B. P., Dawe, R. A. Pore and core-scale displacement mechanisms with spreading and wetting effects during three-phase flow. Paper SPE 39032 Presented at the Latin American and Caribbean Petroleum Engineering Conference, Rio de Janeiro, Brazil, 30 August-3 September, 1997.

Gunstensen, A. K. Lattice-Boltzmann studies of multiphase flow through porous media. Massachusetts, Massachusetts Institute of Technology, 1992.

Guo, Z., Zheng, C., Shi, B. Discrete lattice effects on the forcing term in the lattice Boltzmann method. Physical Review E, 2002, 65(4): 046308.

Gupta, S. Physics-based 3-phase relative permeability for gas-liquid counter-current flow. Paper SPE 210445 Presented at the SPE Annual Technical Conference and Exhibition, Houston, Texas, USA, 3-5 October, 2022.

Hao, L., Cheng, P. Pore-scale simulations on relative permeabilities of porous media by lattice Boltzmann method. International Journal of Heat and Mass Transfer, 2010, 53(9-10): 1908-1913.

He, X., Shan, X., Doolen, G. D. Discrete Boltzmann equation model for nonideal gases. Physical Review E, 1998, 57(1): R13-R16.

Huang, H., Lu, X. Relative permeabilities and coupling effects in steady-state gas-liquid flow in porous media: A lattice Boltzmann study. Physics of Fluids, 2009, 21(9): 092104.

Hui, M. H., Blunt, M. J. Effects of wettability on three-phase flow in porous media. Journal of Physical Chemistry B, 2000, 104(16): 3833-3845.

Hustad, O. S., Ransen, A. G. A consistent correlation for three-phase relative permeabilities and phase pressures based on three sets of two phase data. Paper IOR 1995 Presented at 8th European Symposium on Improved Oil Recovery, Vienna, Austria, 15-17 May, 1995.

Jahanbakhsh, A., Sohrabi, M., Fatemi, S. M., et al. A comparative study of the effect of gas/oil IFT variation on two- and three-phase relative permeability and the performance of WAG injection at laboratory scale. Paper SPE 179571 Presented at the SPE Improved Oil Recovery Conference, Tulsa, Oklahoma, USA, 11-13 April, 2016.

Jerauld, G. R. General three-phase relative permeability model for Prudhoe Bay. SPE Reservoir Engineering, 1997, 12(4): 255-263.

Jerauld, G. R., Rathmell, J. J. Wettability and relative permeability of Prudhoe Bay: A case study in mixed-wet reservoirs. SPE Reservoir Engineering, 1997, 12(1): 58-65.

Ji, M., Kwon, S., Choi, S., et al. Numerical investigation of CO_2-carbonated water-alternating-gas on enhanced oil recovery and geological carbon storage. Journal of CO_2 Utilization, 2023, 74: 102544.

Johnson, E., Bossler, D. P., Bossler, V. O. N. Calculation of relative permeability from displacement experiments. Transactions of the AIME, 1959, 216(1): 370-372.

Kalaydjian, F. J-M. Performance and analysis of three-phase capillary pressure curves for drainage and imbibition in porous media. Paper SPE 24878 Presented at the SPE Annual Technical Conference and Exhibition, Washington, D.C., 4-7 October, 1992.

Kalaydjian, F. J-M., Moulu, J., Vizika, O., et al. Three-phase flow in water-wet porous media: determination of gas/oil relative permeabilities under various spreading conditions. Paper SPE 26671 Presented at the SPE Annual Technical Conference and Exhibition, Houston, Texas, 3-6 October, 1993.

Kalaydjian, F. J-M., Moulu, J-C., Vizika, O., et al. Three-phase flow in water-wet porous media: Gas/oil relative permeabilities for various spreading conditions. Journal of Petroleum Science and Engineering, 1997, 17(3-4): 275-290.

Kantzas, A., Chatzis, I., Dullien, F. A. L. Enhanced oil recovery by inert gas injection. Paper SPE 17379 Presented at the SPE Enhanced Oil Recovery Symposium, Tulsa, Oklahoma, 16-21 April, 1988.

Kianinejad, A., Chen, X., DiCarlo, D. A. The effect of saturation path on three-phase relative permeability. Water Resources Research, 2015, 51(11): 9141-9164.

Kianinejad, A., DiCarlo, D. A. Three-Phase oil relative permeability in water-wet media: A comprehensive study. Transport in Porous Media, 2016, 112(3): 665-687.

Killough, J. Reservoir simulation with history-dependent saturation functions. Society of Petroleum Engineers Journal, 1976, 16(1): 37-48.

Kjosavik, A., Ringen, J., Skjæveland, S. M. Relative permeability correlation for mixed-wet reservoirs. SPE Journal, 2002, 7(1): 49-58.

Kokal, S., Maini, B. B. An improved model for estimating three-phase oil-water-gas relative permeabilities from two-phase oil-water and oil-gas data. Journal of Canadian Petroleum Technology, 1990, 29(2): 105-114.

Kong, D., Gao, Y., Sarma, H., et al. Experimental investigation of immiscible water-alternating-gas injection in ultra-high water-cut stage reservoir. Advances in Geo-Energy Research, 2021, 5(2): 139-152.

Kvanvik, B. A., Skauge, A., Matre, B., et al. Three-phase microemulsion relative permeabilities: Experimental and theoretical consideration. Journal of Petroleum Science and Engineering, 1992, 7(1-2): 105-116.

Land, C. S. Calculation of imbibition relative permeability for two-and three-phase flow from rock properties. Society of Petroleum Engineers Journal, 1968, 8(2): 149-156.

Larsen, J. A., Skauge, A. Methodology for numerical simulation with cycle-dependent relative permeabilities. SPE Journal, 1998, 3(2): 163-173.

Larsen, J. A., Skauge, A. Simulation of the immiscible WAG process using cycle-dependent three-phase relative permeabilities. Paper SPE 56475 Presented at the SPE Annual Technical Conference and Exhibition, Houston, Texas, 3-6 October, 1999.

Leverett, M. C., Lewis, W. B. Steady flow of gas-oil-water mixtures through unconsolidated sands. Transactions of the AIME, 1941, 142(1): 107-116.

Li, T., Long, A., Liu, B., et al. Breakthrough pressure and gas injection development strategies for separation and intercalation gas injection in low-permeability sandstone reservoirs—An example of the E31 reservoir in the Gaaskul field, Qaidam Basin. Petroleum Research, 2021, 42(10): 1364-1372. (in Chinese)

Li, H., Pan, C., Miller, C. T. Pore-scale investigation of viscous coupling effects for two-phase flow in porous media. Physical Review E, 2005, 72(2): 026705.

Liu, H., Zhang, Y., Valocchi, A. J. Lattice Boltzmann simulation of immiscible fluid displacement in porous media: Homogeneous versus heterogeneous pore network. Physics of Fluids, 2015, 27(5): 052103.

Lu, W., Liu, Q., Zhang, Z., et al. Measurement of three-phase relative permeabilities. Petroleum Exploration and Development, 2012, 39(6): 758-763.

Maini, B. B., Kokal, S., Jha, K. Measurements and correlations of three-phase relative permeability at elevated temperatures and pressures. Paper SPE 19677 Presented at the SPE Annual Technical Conference and Exhibition, San Antonio, Texas, 8-11 October, 1989.

Maloney, D. R., Doggett, K., Brinkmeyer, A. D. Special Core Analyses and Relative Permeability Measurement on Almond Formation Reservoir Rocks. Bartlesville, USA, National Institute for Petroleum and Energy Research, 1993.

Maloney, D. R., Honarpour, M. M., Brinkmeyer, A. D. The Effects of Rock Characteristics on Relative Permeability. Bartlesville, USA, National Institute for Petroleum and Energy Research, 1990.

Maloney, D. R., Mahmood, S. M., Honarpour, M. M. The Effects of Viscous Forces on Three-Phase Relative Permeability. Bartlesville, USA, National Institute for Petroleum and Energy Research, 1989.

Marek, B., Hartman, K., McDonald, A. E. Three-phase relative permeability of limestones having bimodal pore-size distribution. Paper SPE 21374 Presented at the Middle East Oil Show, Bahrain, 16-19 November, 1991.

Masihi, M., Javanbakht, L., Horeh, F. B., et al. Experimental investigation and evaluation of three-phase relative permeability models. Journal of Petroleum Science and Engineering, 2011, 79(1-2): 45-53.

Mayberry, D. J., Afsharpoor, A., Kam, S. I. The use of fractional-flow theory for foam displacement in presence of oil. SPE Reservoir Evaluation & Engineering, 2008, 11(4): 707-718.

Moghadasi, L., Guadagnini, A., Inzoli, F., et al. Characterization of two- and three-phase relative permeability of water-wet porous media through X-Ray saturation measurements. Journal of Petroleum Science and Engineering, 2016, 145: 453-463.

Morgan, J. T., Gordon, D. T. Influence of pore geometry on water-oil relative permeability. Journal of Petroleum Technology, 1970, 22(10): 1199-1208.

Moulu, J., Vizika, O., Kalaydjian, F., et al. A new model for three-phase relative permeabilities based on a fractal representation of the porous medium. Paper SPE 38891 Presented at the SPE Annual Technical Conference and Exhibition, San Antonio, Texas, 5-8 October, 1997.

Munkerud, P. K., Hoimyr, O. Gas mobility during three phase flow in a WAG process. Paper IOR 1995 Present at the 8th European Symposium on Improved Oil Recovery, Vienna, Austria, 15-17 May, 1995.

Muqeem, M. A., Bentsen, R. G., Maini, B. B., et al. An improved steady-state technique for three-phase relative permeability measurements. Paper Presented at the Annual Technical Meeting, Calgary, Alberta, 8-11 May, 1993.

Naar, J., Wygal, R. Three-phase imbibition relative permeability. Society of Petroleum Engineers Journal, 1961, 1(4): 254-258.

Oak, M. Three-phase relative permeability of water-wet Berea. Paper SPE 20183 Presented at the SPE/DOE Enhanced Oil Recovery Symposium, Tulsa, Oklahoma, 22-25 April, 1990.

Oak, M. Three-phase relative permeability of intermediate-wet Berea sandstone. Paper SPE 22599 Presented at the SPE Annual Technical Conference and Exhibition, Dallas, Texas, 6-9 October, 1991.

Oren, P. E., Billiotte, J., Pinczewski, W. V. Mobilization of waterflood residual oil by gas injection for water-wet conditions. SPE Formation Evaluation, 1992, 7(1): 70-78.

Oren, P. E., Pinczewski, W. V. The effect of film-flow on the mobilization of waterflood residual oil by gas flooding.

Paper IOR 1991 Presented at the 6th European Symposium on Improved Oil Recovery, Stavanger, Norway, 21-23 May, 1991.

Perez-Carrillo, E. R., Zapata-Arango, J. F., Santos-Santos, N. A new method for the experimental determination of three-phase relative permeabilities. CT&F-Ciencia Tecnología y Futuro, 2008, 3(4): 23-43.

Petersen, E., Lohne, A., Vatne, K. O., et al. Relative permeabilities for two-and three phase flow processes relevant to the depressurization of the Statfjord field. Paper Presented at the International Symposium of the Society of Core Analysts. Abu Dhabi, UAE, 29 October-2 November, 2008.

Sahni, A., Burger, J., Blunt, M. Measurement of three phase relative permeability during gravity drainage using CT. Paper SPE 39655 Presented at the SPE/DOE Improved Oil Recovery Symposium, Tulsa, Oklahoma, 19-22 April, 1998.

Salathiel, R. Oil recovery by surface film drainage in mixed-wettability rocks. Journal of Petroleum Technology, 1973, 25(10): 1216-1224.

Saraf, D. N., Batycky, J. P., Jackson, J. H., et al. An experimental investigation of three-phase flow of water-oil-gas mixtures through water-wet sandstones. Paper SPE 10761 Presented at the SPE California Regional Meeting, San Francisco, California, 24-26 March, 1982.

Sarem, A. Three-phase relative permeability measurements by unsteady-state method. Society of Petroleum Engineers Journal, 1966, 6(3): 199-205.

Sarma, H. K., Maini, B. B., Jha, K. N. An unsteady-state technique for three-phase relative permeability measurements. Journal of Canadian Petroleum Technology, 1994, 33(2): 27-33.

Schmid, C. The wettability of petroleum rocks and results of experiments to study effects of variations in wettability of core samples. Erdoel Kohle, 1964, 17(8): 605-609.

Shahrokhi, O., Fatemi, M., Sohrabi, M., et al. Assessment of three phase relative permeability and hysteresis models for simulation of water-alternating-gas WAG injection in water-wet and mixed-wet systems. Paper SPE 169170 Presented at the SPE Improved Oil Recovery Symposium, Tulsa, Oklahoma, USA, 12-16 April, 2014.

Shahverdi, H., Sohrabi, M. An improved three-phase relative permeability and hysteresis model for the simulation of a water-alternating-gas injection. SPE Journal, 2013, 18(5): 841-850.

Shahverdi, H., Sohrabi, M. Relative permeability characterization for water-alternating-gas injection in oil reservoirs. SPE Journal, 2016, 21(3): 799-808.

Shahverdi, H., Sohrabi, M. A mechanistic model for prediction of three-phase flow in petroleum reservoirs. Journal of Petroleum Science and Engineering, 2017, 157: 507-518.

Shahverdi, H., Sohrabi, M., Fatemi, M., et al. Evaluation of three-phase relative permeability models for WAG injection using water-wet and mixed-wet core flood experiments. Paper SPE 143030 Presented at the SPE EUROPEC/EAGE Annual Conference and Exhibition, Vienna, Austria, 23-26 May, 2011a.

Shahverdi, H., Sohrabi, M., Fatemi, M., et al. Three-phase relative permeability and hysteresis effect during WAG process in mixed wet and low IFT systems. Journal of Petroleum Science and Engineering, 2011b, 78(3-4): 732-739.

Shan, X., Chen, H. Lattice Boltzmann model for simulating flows with multiple phases and components. Physical Review E, 1993, 47(3): 1815-1819.

Shelton, J. L., Yarborough, L. Multiple phase behavior in porous media during CO_2 or rich-gas flooding. Journal of Petroleum Technology, 1977, 29(9): 1171-1178.

Siddiqui, S., Hicks, P. J., Grader, A. S. Verification of Buckley-Leverett three-phase theory using computerized tomography. Journal of Petroleum Science and Engineering, 1996, 15(1): 1-21.

Siddiqui, S., Yang, J., Ahmed, M. Dynamic displacement measurement of three-phase relative permeabilities in Berea sandstone cores. Paper SPE 49306 Presented at the SPE Annual Technical Conference and Exhibition, New Orleans, Louisiana, 27-30 September, 1998.

Singh, M., Mani, V., Honarpour, M. M., et al. Comparison of viscous and gravity dominated gas-oil relative permeabilities. Journal of Petroleum Science and Engineering, 2001, 30(2): 67-81.

Skauge, A., Larsen, J. A. Three-phase relative permeabilities and trapped gas measurements related to WAG processes. Paper SCA 9421 Presented at the Proceedings of the International Symposium of the Society of Core Analysts, Stavanger, Norway, 12-14 September, 1994.

Spencer, T., Halliday, I., Care, C. M. Lattice Boltzmann equation method for multiple immiscible continuum fluids. Physical Review E, 2010, 82(6): 066701.

Spiteri, E. J., Juanes, R. Impact of relative permeability hysteresis on the numerical simulation of WAG injection. Journal of Petroleum Science and Engineering, 2006, 50(2): 115-139.

Spiteri, E. J., Juanes, R., Blunt, M. J., et al. Relative-permeability hysteresis: trapping models and application to geological CO_2 sequestration. Paper SPE 96448 Presented at the SPE Annual Technical Conference and Exhibition, Dallas, Texas, 9-12 October, 2005.

Stone, H, L. Probability model for estimating three-phase relative permeability. Journal of Petroleum Technology, 1970, 22(2): 214-218.

Stone, H. L. Estimation of three-phase relative permeability and residual oil data. Journal of Canadian Petroleum Technology, 1973, 12(4): 53-61.

Swift, M. R., Orlandini, E., Osborn, W. R., et al. Lattice Boltzmann simulations of liquid-gas and binary fluid systems. Physical Review E, 1996, 54(5): 5041-5052.

Tang, J. Y., Castaneda, P., Marchesin, D., et al. Three-phase fractional-flow theory of foam-oil displacement in porous media with multiple steady states. Water Resources Research, 2019, 55(12): 10319-10339.

Vizika, O., Lombard, J.-M. Wettability and spreading: Two key parameters in oil recovery with three-phase gravity drainage. SPE Reservoir Engineering, 1996, 11(1): 54-60.

Wang, G., Pickup, G. E., Sorbie, K. S., et al. Detailed assessment of compositional and interfacial tension effects on the fluid behaviour during immiscible and near-miscible CO_2 continuous and WAG displacements. Transport in Porous Media, 2020, 131(3): 805-830.

Wei, B., Huang, H., Hou, J., et al. Study on the meniscus-induced motion of droplets and bubbles by a three-phase Lattice Boltzmann model. Chemical Engineering Science, 2018, 176: 35-49.

Welge, H. J. A simplified method for computing oil recovery by gas or water drive. Journal of Petroleum Technology, 1952, 4(4): 91-98.

Wilberforce, T., Olabi, A., Sayed, E. T., et al. Progress in carbon capture technologies. Science of The Total Environment, 2021, 761: 143203.

Xie, C., Lei, W., Balhoff, M. T., et al. Self-adaptive preferential flow control using displacing fluid with dispersed polymers in heterogeneous porous media. Journal of Fluid Mechanics, 2021, 906: A10.

Xie, C., Lei, W., Wang, M. Lattice Boltzmann model for three-phase viscoelastic fluid flow. Physical Review E, 2018, 97(2): 023312.

Xie, C., Xu, K., Mohanty, K., et al. Nonwetting droplet oscillation and displacement by viscoelastic fluids. Physical Review Fluids, 2020, 5(6): 063301.

Xie, C., Xu, K., Qi, P., et al. A new mechanism of viscoelastic fluid for enhanced oil recovery: Viscoelastic oscillation. Advances in Geo-Energy Research, 2022, 6(3): 267-268.

Yang, Y., Zhou, Y., Blunt, M. J., et al. Advances in multiscale numerical and experimental approaches for multiphysics problems in porous media. Advances in Geo-Energy Research, 2021, 5(3): 233-238.

Yu, Z., Fan, L. -S. Multirelaxation-time interaction-potential-based lattice Boltzmann model for two-phase flow. Physical Review E, 2010, 82(4): 046708.

Yu, Y., Liang, D., Liu, H. Lattice Boltzmann simulation of immiscible three-phase flows with contact-line dynamics. Physical Review E, 2019, 99(1): 013308.

Zankoor, A., Khishvand, M., Piri, M. In-Situ capillary pressure and its interrelationships with flow characteristics during steady-state three-phase flow in water-wet Berea Sandstone. Water Resources Research, 2022, 58(12): e2022WR032976.

Zhang, C., Ding, H., Gao, P., et al. Diffuse interface simulation of ternary fluids in contact with solid. Journal of Computational Physics, 2016, 309: 37-51.

Zhang, D., Li, S., Jiao, S., et al. Relative permeability of three immiscible fluids in random porous media determined by the lattice Boltzmann method. International Journal of Heat and Mass Transfer, 2019, 134: 311-320.

Zhang, G., Yao, G., Li, J., et al. A new experimental method for measuring the three-phase relative permeability of oil, gas, and water. Journal of Petroleum Science and Engineering, 2018, 170: 611-619.

Zhou, D., Blunt, M. J. Wettability effects in three-phase gravity drainage. Journal of Petroleum Science and Engineering, 1998, 20(3-4): 203-211.

Zhou, Z., Huang, J. Study of single-component two-phase free energy lattice Boltzmann models using various equations of state. Physics of Fluids, 2023, 35(4): 042116.

Zhu, X., Chen, L., Wang, S., et al. Pore-scale study of three-phase displacement in porous media. Physics of Fluids, 2022a, 34(4): 043320.

Zhu, W., Liu, Y., Shi, Y., et al. Effect of dynamic threshold pressure gradient on production performance in water-bearing tight gas reservoir. Advances in Geo-Energy Research, 2022b, 6(4): 286-295.

Zhu, X., Wang, S., Feng, Q., et al. Pore-scale numerical prediction of three-phase relative permeability in porous media using the lattice Boltzmann method. International Communications in Heat and Mass Transfer, 2021, 126: 105403.

Zuo, L., Chen, Y., Zhou, D., et al. Three-phase relative permeability modeling in the simulation of WAG injection. SPE Reservoir Evaluation & Engineering, 2014, 17(3): 326-339.